Section 2

Data sets, diagnostic and dynamical investigations, statistical postprocessing, multi-year reanalyses and associated studies

FROST-2014 Field Campaign

Dmitry Kiktev, Hydrometcentre of Russia/Roshydromet
e-mail: dkiktev@mail.ru

The WWRP RDP/FDP FROST-2014 (FROST - Forecast and Research in the Olympic Sochi Testbed) is connected to the XXII Olympic and XI Paralympic Winter Games in Sochi and targeted at advancement and demonstration of state-of-the-art nowcasting and short-range forecasting systems for winter conditions in mountainous terrain. The list of the international project participants includes the mesoscale modeling consortia COSMO and HIRLAM/ALADIN, the Central Institute for Meteorology and Geodynamics (Austria), Environment Canada, the Finnish Meteorological Institute, the National Oceanic and Atmospheric Administration of the United States and the Korea Meteorological Administration.

For purposes of weather analysis, forecasting and forecast verification about forty automatic meteorological stations were installed in the region of Olympics. For majority of the stations the sampling interval did not exceed 10 minutes. For some stations and variables it was enhanced to 1 minute. C-band dual polarization Doppler weather radar was installed on Akhun mountain in Sochi. Wind profiler, two temperature profilers and two Micro Rain Radars supplemented the network. During the Olympic winter the frequency of upper air soundings in Sochi was enhanced to 4 times/day. Additional observations were provided by the neighbourhood countries – Armenia, Turkey and Ukraine. Spatial snow measurements (intensity, depth, fresh snow density, precipitation type and size of crystals) were taken by the local avalanche protection troop.

Six nowcasting systems (model-based, radar tracking and combined nowcasting systems) and seven deterministic mesoscale NWP systems contributed to FROST-2014 (see Annex 1). Several models were implemented for region of the Olympics with grid spacing of 1 km or finer (down to 250 m in GEM system of the Environment Canada). Six ensemble prediction systems (including two convection permitting ones) participated in the project. The project operational forecasts were deeply integrated into the system of meteorological support of the Olympics. A kind of super-ensemble with rapid update cycle and adjustment to the latest observations both for nowcasting and short-range forecasting intervals was implemented and served as a first guess for the Olympic forecasters (that might be considered as one of the project social impacts along with capacity building and transfer of technologies).

With the closure of the Olympics in March 2014 the project field campaign was mostly over. Quite few systematic trials of multiple high-resolution forecasting systems in mountains are known so far due to the lack of appropriate observations and coordinated forecasting activities. In this respect FROST-2014 provides a valuable information resource for mesoscale predictability studies, development and validation of forecasting systems over complex terrain.
The FROST-2014 information archive of observations and forecasts is intended to be a part of the project legacy for the international research community. Today the focus of FROST-2014 activities is switched to analysis of results of the field campaign.

Relative variations of temperature and aerosol concentration in the atmosphere from Antarctic ice cores

I.I. Mokhov, V.A. Bezverkhny, I.S. Larkina

A.M. Obukhov Institute of Atmospheric Physics RAS

mokhov@ifaran.ru

Relative variations of temperature and aerosol concentration in the atmosphere from the Vostok (over the past 420 ka) [1] and EPICA Dome C (EDC, over the past 800 ka) [2] Antarctic ice cores are analyzed with the use of different cross-wavelet methods [3,4] (see also [5-7]).

Figure 1 shows different modes for variations of temperature (T [^{o}C], bold curves) and aerosol (mineral dust) concentration (dust [ppb], thin curves) in the atmosphere from EDC ice core records: a) 100 ka modes, b) 41 ka modes. These modes are corresponding to Milankovich periods. According to Fig. 1a, variations in dust concentration lag behind those in temperature for 100 ka modes. Figure 1b for 41 ka modes shows opposite in sign phase shifts between variations in dust concentration and temperature.

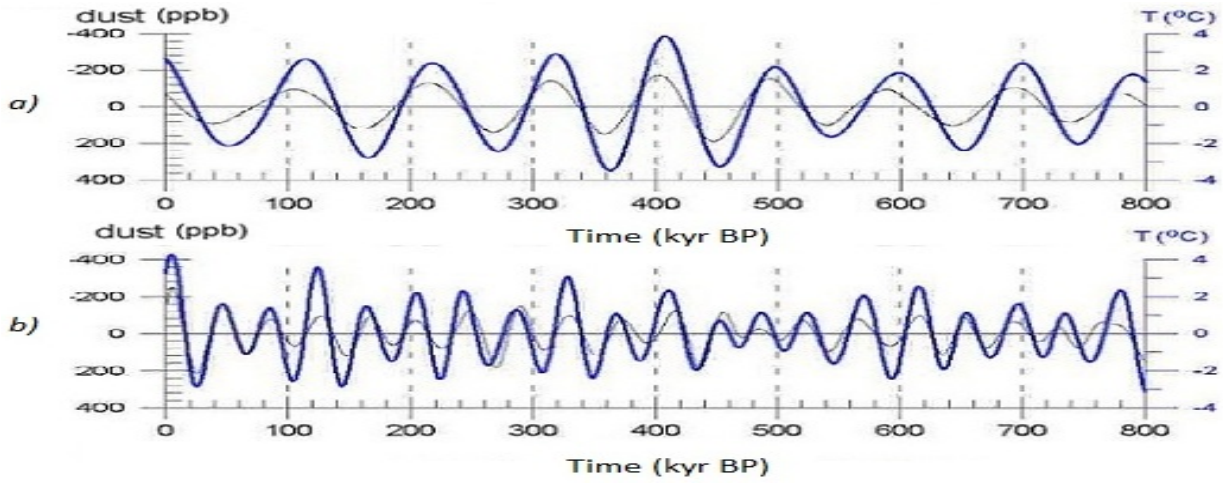

Figure 1. Different modes for variations of temperature T [^{o}C] (bold curves) and aerosol (mineral dust) concentration (dust [ppb], thin curves) in the atmosphere from EDC ice core records: a) 100 ka modes, b) 41 ka modes.

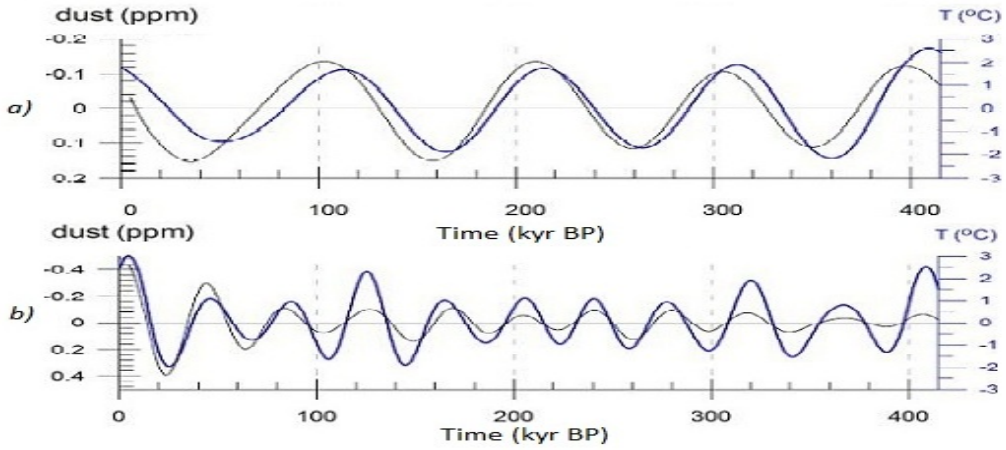

Figure 2. Different modes for variations of temperature (T [^{o}C], bold curves) and aerosol (continental dust) concentration (dust [ppm], thin curves) in the atmosphere from Vostok ice core records: a) 100 ka modes, b) 41 ka modes.

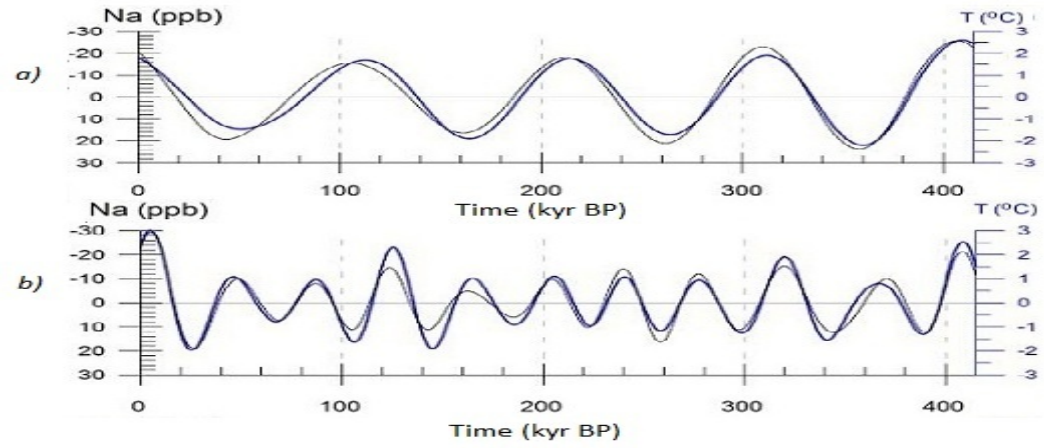

Figure 3. Different modes for variations of temperature (T [^{o}C], bold curves) and marine aerosol concentration (Na [ppb], thin curves) in the atmosphere from Vostok ice core records: a) 100 ka modes, b) 41 ka modes.

Figure 2 and Figure 3 show different modes for variations of temperature and continental dust (Fig. 2) and marine aerosol (Fig. 3) concentration in the atmosphere from Vostok ice core records: a) 100 ka modes, b) 41 ka modes. According to Fig. 2a and Fig. 3a, variations in continental and marine aerosol concentration lag behind those in temperature for 100 ka modes while modes with the period 41 ka display opposite in sign phase shifts between variations in atmospheric aerosol concentration and temperature.

Overall, the results obtained with the use of different methods of cross-wavelet analysis [3-5] reveal the phase lag of temperature variations relative to variations of aerosol concentration for the modes with a period of about 40 ka or less.

References

1. Petit J.R., Jouzel J., Raynaud D. et al., 1999: Climate and atmospheric history of the past 420000 years from the Vostok ice core, Antarctica. *Nature*, **399**, 429-436.
2. EPICA community members, 2004: Eight glacial cycles from an Antarctic ice core. *Nature*, **429**, 623-628.
3. Bezverkhny V.A., 2001: Developing the wavelet-transform method for analysis of geophysical data. *Izvestiya, Atmos. Oceanic Phys.*, **37**(5), 584-591.
4. Grinsted A., Moore J.C., Jevrejeva S., 2004: Application of the cross wavelet transform and wavelet coherence to geophysical time series. *Nonlin. Processes Geophys.*, **11**, 561-566.
5. Mokhov I.I., Bezverkhny V.A., Karpenko A.A., 2002: Mutual dynamics of atmospheric components and climatic characteristics during last 420,000 years from Vostok ice core. *Research Activ. Atmos. Oceanic Model*., WMO/TD-No.1105, 2.17-2.18.
6. Mokhov I.I., Bezverkhny V.A., Karpenko A.A., 2005: Diagnosis of relative variations in atmospheric greenhouse gas contents and temperature from Vostok Antarctic ice core paleoreconstructions. *Izvestiya, Atmos. Oceanic Phys.*, **41**(5), 523-592.
7. Mokhov I.I., Bezverkhny V.A., Karpenko A.A., 2010: Relative changes in temperature and concentration of greenhouse gases in the atmosphere from paleoreconstructions for last 800 ka. In: Extreme Environmental Hazards and Catastrophes. V. I. Evaluation and Ways to Reduce Negative Consequences of Extreme Environmental Phenomena. RAS, Moscow. 312-319. (in Russian)

Drought risk in the North Eurasian regions: assessment of El-Nino effects

Igor I. Mokhov and Alexandr V. Timazhev

A.M. Obukhov Institute of Atmospheric Physics RAS
mokhov@ifaran.ru

We analyzed the probability of drought conditions in the North Eurasian regions and assessed El-Nino/Southern Oscillation (ENSO) effects [1]. Based on observations [2] for the period 1891-2013, we analyzed the spring-summer (May-July) anomalies of surface air temperature (SAT) δT and precipitation δP, as well as of drought index D in the mid-latitudes of the European (ER) and Asian (AR) parts of Russia .

To estimate the El-Nino/La-Nina effects, we used their indices based on sea surface temperature (SST) in the Niño-3 (150°–90°W, 4°N–4°S), Nino-3,4 (170°–120°W, 4°N–4°S) and Nino-4 (160°E–150°W, 4°N–4°S) regions in the equatorial latitudes of the Pacific Ocean (ftp://www.coaps.fsu.edu/ pub/JMA_SST_Index/). The El-Nino (E) and La-Nina (L) phases were distinguished using 5-month moving averages of the SST anomaly in the Nino-3 region (JMA index). El-Nino (warm) and La-Nina (cold) phases were defined by the index values of at least 0.5°C and at most –0.5°C, respectively, over six consecutive months (including October–December). All other cases were considered as neutral phases (N).

The beginning of 2015 in the El-Nino phase was characterized by the highest positive anomalies in the Nino-4 region and we present here the results with Nino-4 as the El-Nino index. According to ensemble model forecasts, the probability that El-Nino phase will persist till the end of this year is about 60% (more than 70% for May-July and June-August). The corresponding probability for neutral and La-Nina phases is estimated at about 30% and 10%, correspondingly (http://iri.columbia.edu).

Table 1 shows the probabilities of positive spring–summer temperature anomalies δT in the ER and AR for different El-Nino phase transitions estimated with the use of the Nino-4 index. The transitions characterized by the highest probability of temperature anomalies, including extreme ones (δT > 1°C), for the ER and AR are shown in bold. It should be noted that the $E \rightarrow E$ transition expected in 2015 is characterized by the highest probability (0.71) of extremely high temperature in May-July over the AR with a low risk of high temperatures for the ER.

Table 1. Probability of different surface temperature anomalies (δT) in the ER (and AR) in May-July for different ENSO phases (characterized by the Nino-4 index) based on observations for 1891–2013

δT	$N\rightarrow$ $n=67$			$E\rightarrow$ $n=28$			$L\rightarrow$ $n=28$		
	$N\rightarrow E$ n=17	$N\rightarrow L$ n=9	$N\rightarrow N$ n=41	$E\rightarrow E$ n=7	$E\rightarrow L$ n=8	$E\rightarrow N$ n=13	$L\rightarrow E$ n=4	$L\rightarrow L$ n=10	$L\rightarrow N$ n=14
>0	0.41 (0.47)	0.56 (0.44)	0.63 (0.61)	0.29 (**0.71**)	**0.88** (0.62)	0.54 (0.38)	0.50 (0.50)	0.40 (0.50)	0.43 (0.57)
	0.53 (0.51)			**0.57** (**0.57**)			0.44 (0.52)		
>1 K	0.12 (0.24)	0.22 (0.11)	0.22 (0.22)	0.14 (**0.71**)	**0.50** (0.12)	0.31 (0.15)	0.25 (0.25)	0.20 (0.20)	0.21 (0.29)
	0.19 (0.19)			**0.32** (**0.33**)			0.22 (0.25)		

Table 2 presents the probability of negative precipitation anomalies in the ER and AR (δP) in May–July for different ENSO phase transitions estimated with the use of Nino-4 index.

Table 2. Probability of negative precipitation anomalies (δP) in the ER (and AR) in May–July for different ENSO phases (characterized by the Nino-4 index) from observations for 1891–2013

δP	$N\rightarrow$ $n = 67$			$E\rightarrow$ $n = 28$			$L\rightarrow$ $n = 28$		
	$N\rightarrow E$ n=17	$N\rightarrow L$ n=9	$N\rightarrow N$ n=41	$E\rightarrow E$ n=7	$E\rightarrow L$ n=8	$E\rightarrow N$ n=13	$L\rightarrow E$ n=4	$L\rightarrow L$ n=10	$L\rightarrow N$ n=14
< 0	0.47 (0.35)	0.56 (0.33)	0.51 (0.34)	0.29 (0.57)	0.38 (0.50)	0.54 (0.62)	0.50 (**0.75**)	**0.60** (0.50)	0.43 (0.36)
		0.51 (0.34)			0.40 (**0.56**)			**0.51** (0.54)	

Table 3 shows probability of different drought conditions (index D) in the ER (and AR) in May-July for different ENSO phase transitions with the use of the Nino-4 index.

Table 3. Probability of different drought conditions (index D) in the ER (and AR) in May-July for different ENSO phases (characterized by the Nino-4 index) from observations for 1891–2013

D	$N\rightarrow$ $n = 67$			$E\rightarrow$ $n = 28$			$L\rightarrow$ $n = 28$		
	$N\rightarrow E$ n=17	$N\rightarrow L$ n=9	$N\rightarrow N$ n=41	$E\rightarrow E$ n=7	$E\rightarrow L$ n=8	$E\rightarrow N$ n=13	$L\rightarrow E$ n=4	$L\rightarrow L$ n=10	$L\rightarrow N$ n=14
≥20%	0.24 (0.35)	**0.56** (0.33)	0.51 (0.29)	0.43 (**0.71**)	0.50 (0.38)	0.46 (0.38)	0.25 (0.50)	0.30 (0.30)	0.29 (0.36)
		0.44 (0.32)			**0.46** (**0.49**)			0.28 (0.39)	
≥30%	0.12 (0.06)	0.22 (0)	0.27 (0.20)	0 (**0.43**)	**0.38** (0.12)	0.31 (0.23)	0.25 (0.25)	0.30 (0.20)	0.21 (0.21)
		0.20 (0.09)			0.23 (**0.26**)			**0.25** (0.22)	

According to Table 3 the $E\rightarrow E$ transition expected in 2015 is characterized by the high risk of drought conditions in May-July in AR. Severe drought conditions ($D \geq 30\%$) in AR were realized three times in seven $E\rightarrow E$ transitions since 1891.

References

1. Mokhov I.I. and A.V. Timazhev (2013) Climatic anomalies in Eurasia from El-Nino/La-Nina effects. *Doklady Earth Sci.,* **453**(1), 1141-1144.
2. Meshcherskaya A.V., V.M. Mirvis, and M.P. Golod (2011) The drought in 2010 against the background of multiannual changes in aridity in the major grain-producing regions of the European part of Russia. *Tr. MGO,* **563**, 94–121 (in Russian)

Multidecadal climate variations:
Assessment of their influence on temperature trends

Igor I. Mokhov and Vyacheslav A. Bezverkhny

A.M. Obukhov Institute of Atmospheric Physics RAS
mokhov@ifaran.ru

General warming during the last century is accompanied by remarkable quasi-cyclic natural climate variations with a significant role of multidecadal variations with a period of about 6 decades. The analysis of surface air temperature (SAT) observations in the 19th century shows the key role of atmospheric CO_2 in the centennial global climate changes [1-4]. According to [1], more than 3/4 of the global SAT variance is due to CO_2. The natural 60-year mode and all the remaining factors are responsible for 1/20 and 1/6 of the global SAT variance, respectively. For the Arctic, the appropriate CO_2 contribution is assessed at less than 1/2, while that of the 60-year mode is about 1/6. The contribution of variations in solar radiation ("solar activity") was estimated as insignificant (less than 1%).

What is the quantitative influence of the natural 60-year mode on the contemporary SAT trends? Figure 1 shows an example of extrapolation of SAT variations in the Northern Hemisphere (NH) from the GISS data (http://data.giss.nasa.gov/gistemp/) up to the 22nd century. Similar estimates can be made for the Arctic with the most rapid climate changes [4].

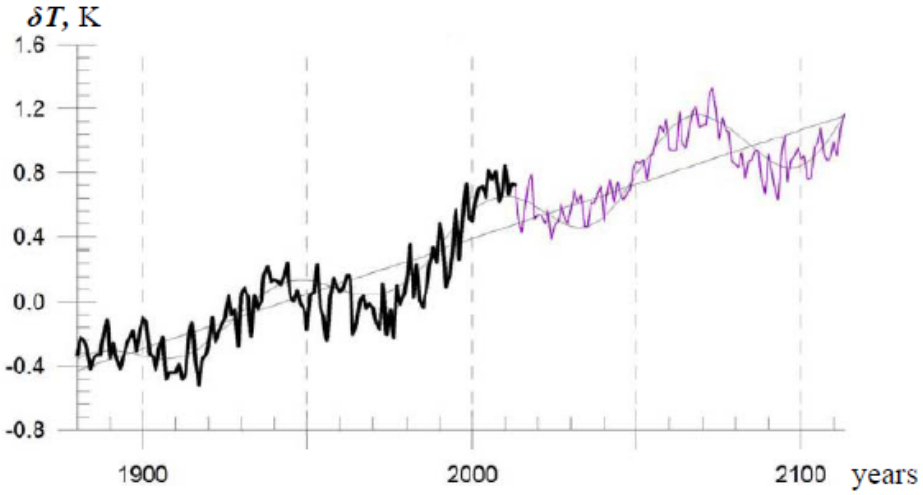

Figure 1. Extrapolation of SAT variations in the Northern Hemisphere from the GISS data (black curve) up to the 22nd century (violet curve). Variations around the linear trend line which characterize the 60-year mode are shown in grey.

Taking into account the current phase of the 60-year mode against the background of the centennial warming, a slowdown of warming or even a local cooling should be expected in the next two decades, followed by the amplification of warming at regional and global scales. Let us consider the simplest case of SAT ($T(t)$) harmonic oscillation with the period T_0 (60 years) and the amplitude ΔT against the background of the centennial SAT trend $(dT/dt)_c$:

$$T(t) = T_c + (dT/dt)_c t + \Delta T \sin(2\pi t/T_0 + \varphi_0). \quad (1)$$

According to (1), the maximum and minimum SAT trends are

$$(dT/dt)_{max} = (dT/dt)_c + 2\pi(\Delta T/T_0)$$

and

$$(dT/dt)_{min} = (dT/dt)_c - 2\pi(\Delta T/T_0),$$

respectively. In such a case, the necessary and sufficient condition for the absence of a time interval with cooling is as follows [4]:

$$\left(\frac{dT}{dt}\right)_c / \left(\frac{2\pi\Delta T}{T_0}\right) \geq 1. \quad (2)$$

For the whole Arctic, the amplitude of the multidecadal climate oscillations with a period of about 60 years can be estimated at about 0.3 K (with a maximum in the first decade of the 21st century) with the uncertainty ranging from 0.2 K to 0.4 K . The centennial SAT trend in the Arctic $(dT/dt)_A$ was estimated at 2.4 K/(100 years). For the validity of (2), the amplitude $(\Delta T)_A$ of SAT oscillations with a 60-year period T_0 in the Arctic should not exceed $(dT/dt)_A (T_0/2\pi)$=0.23 K [4].

In the Northern Hemisphere the corresponding amplitude of SAT oscillations with a period of about 60 years (with a peak in the first decade of the 21st century) is about 0.2 K (with a minimum at about 0.1 K). The centennial NH SAT trend $(dT/dt)_{NH}$ was estimated at 1.0 K/(100 years). For the validity of (2), the amplitude $(\Delta T)_{NH}$ of the NH SAT oscillations with a period T_0 of about 60 years should not exceed $(dT/dt)_A (T_0/2\pi)$=0.1 K [4].

According to the estimates, we should expect not only the hiatus effects in the global warming but also temporary cooling during the next two decades.

References

1. IPCC (2013): Climate Change 2013: The Physical Science Basis. Contribution of Working Group I to the Fifth Assessment Report of the Intergovernmental Panel on Climate Change. T.F. Stocker, D. Qin, G.-K. Plattner et al. (eds.). Cambridge Univ. Press, Cambridge / N.Y., 1535 p.
2. Gruza G.V., Rankova E.Y. (2012) Observed and Expected Climate Changes in Russia: Air Temperature. VNIIGMI MTsD, Obninsk, 194 p.(in Russian)
3. Mokhov I.I., Smirnov D.A., Karpenko A.A. (2012). Assessments of the correlation between variations in the global surface air temperature and different natural and anthropogenic factors based on the data of observations. *Doklady Earth Sci.,* **443**(1), 381-387.
4. Mokhov I.I. (2015) Contemporary climate changes in the Arctic. *Herald of the Russian Academy of Sciences,* **85**(3).

A role of storm activity in formation of high air pollution

N.V. Pankratova and M.G. Akperov

A.M. Obukhov Institute of Atmospheric Physics, RAS, Moscow, Russia
e-mail: n_pankratova@list.ru

Spatial and temporal variability of gas impurities at different scales was analyzed using measurements at IAP RAS stations and the data of TROICA expeditions (TRanscontinental Observations Into the Chemistry of the Atmosphere). The experiments were conducted annually from 1995 to 2001 and from 2004 to 2012. Two specialized railway cars (a mobile laboratory) were created with the goal to perform continuous measurements of gas and aerosol content in the atmosphere as well as of radiation and meteorological parameters (Pankratova et al., 2011). Thirteen experiments have been made since 1995, including eleven ones when measurements were held along the Trans-Siberian Railway (Moscow-Vladivostok). This paper analyzes large-scale spatial and temporal variations of ground-level concentrations of O_3, NO and NO_2 obtained during observations made between Moscow and Vladivostok. The results of the first experiments have been already published in (Pankratova et al., 2011; Gurjar et al., 2008), subsequent observations gave an opportunity to clarify and supplement the earlier conclusions.

Long-term series of observations enable correct assessment of linear trends in statistical analysis of temporal variability of gas components. Synoptic information and modern reanalysis data were used to take into account the effect of photochemical and dynamic atmospheric processes on the chemical composition of surface air. An automated method of identification of extratropical cyclones and anticyclones was developed to explore and systematize synoptic conditions. Characteristics of extratropical cyclones and anticyclones, including the number, size and intensity were investigated. The relation between the characteristics of storm-track activity and the surface air composition in Central Russia (IAP RAS stations) and in Central Siberia (Zotino) was analyzed. The contribution of various synoptic processes in terms of accumulation and dispersion admixtures was studied. This work helps to clarify the previously developed methods for forecasting extreme ecological situations.

For example, the accumulation of impurities in the surface layer of the atmosphere was observed during extremely hot summer of 2010 in the central regions of Russia. Because of this the concentration of many pollutants significantly exceeded the MAC (maximum allowable concentration) (Fig. 1).

A similar situation was observed in Siberia during the summer of 2012, when catastrophic fires were observed in the region. In both cases, the reason for such strong fires was quasi-stationary anticyclones, which contributed to the establishment of hot dry weather. It is obvious that the storm activity in the atmosphere played a key role in the formation of extreme situations.

This work has been funded by RFBR № 15-55-04097, 15-35-21061, 14-05-31078.

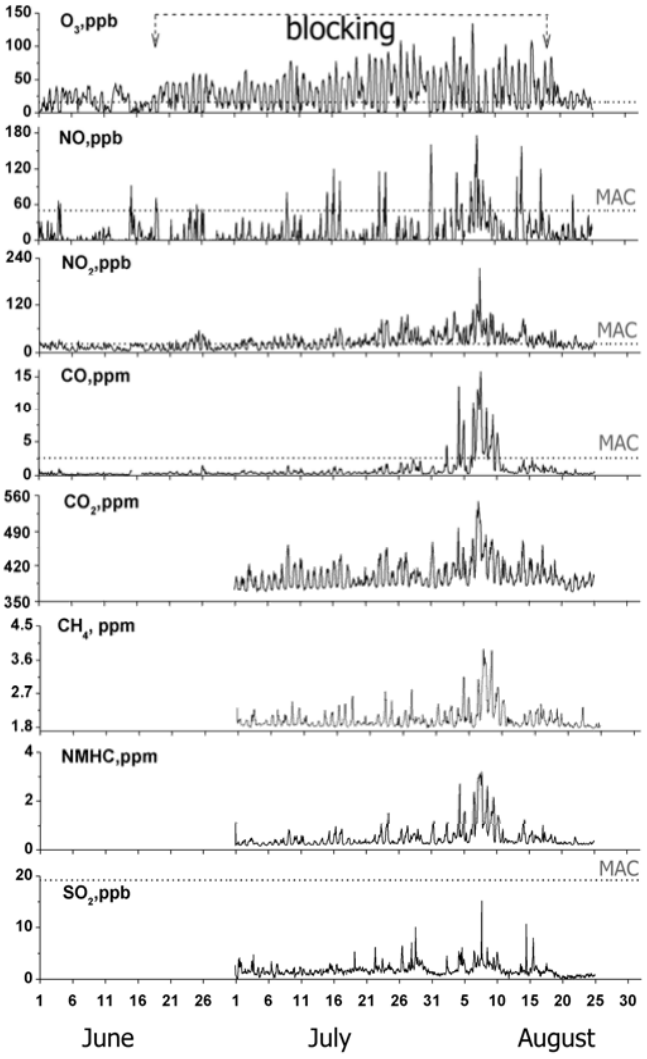

Figure 1. Hourly average concentration of ozone, NO, NO_2, CO, CO_2, CH_4, NMHC, and SO_2 at the Moscow IAP RAS station during the extremely hot summer of 2010. The dotted line shows MAC.

References

Pankratova N.V., Elansky N.F., Belikov I.B., Lavrova O.V., Skorokhod A.I., Shumsky R.A. Ozone and nitric oxides in the surface air over northern Eurasia according to observational data obtained in TROICA experiments. Izvestiya. Atmospheric and Oceanic Physics. 2011. T. 47. № 3. C. 313-328.

Gurjar B. R.; Butler T. M.; Lawrence M. G.; Lelieveld J. Evaluation of emissions and air quality in megacities. Atmos. Environ. 2008, 42, 1593–1606.

The Environmental Modeling Center's Model Evaluation Group

Glenn White, Geoffrey Manikin and Corey Guastini
Environmental Modeling Center
National Centers for Environmental Prediction
NWS/NOAA/DOC
College Park, MD 20740
USA
Glenn.White@noaa.gov

The Environmental Modeling Center (EMC) Model Evaluation Group (MEG) formed in the spring of 2012. Inspired by ongoing model evaluation efforts at the European Center for Medium-Range Weather Forecasts (ECMWF), the MEG's goal was to evaluate EMC model performance in a more comprehensive and organized way than had been previously done. The MEG has been a major success in its first three years; several model problems and errors have been noted, brought to the attention of modeling teams and customers, and then thoroughly investigated by developers. Many of the problems, such as the GFS cold/wet bias, SREF initialization, and the initialization of snow cover in several EMC models, have been corrected or at least mitigated in operations. The MEG has also performed thorough post-mortems of high-impact and sometimes poorly-forecast events such as Superstorm Sandy, the June 2012 Ohio Valley-Mid-Atlantic derecho and recent winter storms. Lines of communication have been opened between EMC and the National Centers, the NWS offices, and private customers to alert them of model biases and issues and provide a forum for users to report problems they have seen in EMC forecast systems.

The MEG currently monitors the models in the short (1-3 day) and medium (day 4 and beyond) range periods. In the short-range, the North American Mesoscale (NAM) and its nests, the Short Range Ensemble Forecast (SREF) system, the Rapid Refresh (RAP) and the High-Resolution Rapid Refresh (HRRR), the High-Resolution Windows (HIRESW), and the Hurricane WRF (HWRF) are closely watched. In the medium-range, the GFS, the ECMWF model, the Global Ensemble Forecast System (GEFS), and other international models are evaluated.

The evaluations consist of day-to-day monitoring of real-time forecasting issues and post-mortems of major events as well as reviewing longer-term statistical measures and regional and global mean and anomaly fields. The short-range evaluations have focused primarily over CONUS, while the medium-range evaluations have focused primarily over North America, but with some limited examination of the entire globe. Both have made extensive use of existing verification and graphics within EMC and in the broader community.

As the field has become familiar with the existence of the MEG, the frequency of customers coming to the MEG with inquiries or requests for examinations of cases/issues has rapidly increased. The MEG assisted with evaluations of parallel versions of models being prepared for implementation.

The current effort features weekly teleconference briefings. The MEG pays considerable attention to NWS regional and local forecasters and to other NCEP centers; people from other NCEP centers, NWS regional and field offices and other agencies in NOAA have made presentations in MEG and people from the private sector participate.

The primary target of the MEG is enhanced model development. Its purpose is to evaluate EMC models and help model developers improve the models. Another purpose is to provide information to the users about the performance of the EMC models and about proposed changes to the models.

It is hoped that in the future the MEG will help develop a more integrated science-technology structure in which EMC forecast system developers work as one team with NWS forecasters to develop improved forecasts.

The NCEP 65+ Year Reanalysis Observation Database

***J.S.Woollen** IMSG/EMC/NCEP/NOAA (jack.woollen@noaa.gov)*

NCEP partnered with NCAR, with contributions from other NWP research centers, to produce the first long term (50 years, 1948-1998) global reanalysis product during the 1990's. The database setup and data assimilation component carried out at NCEP was ongoing through the years 1993-2000. The project was known as the NCEP/ NCAR Global Reanalysis (NNGR), or GR1. The observation preparation and preprocessing requirement for this project was significant. The bits and pieces of the data were stored in many different places and formats. The data rescue group of ~10 people at NCAR spent many man years cleaning up and time checking archived datasets and sending them to NCEP. Diagrams below, for example, show the major components of the PILOT/TEMP and the SYNOP datasets, 1948-1997.

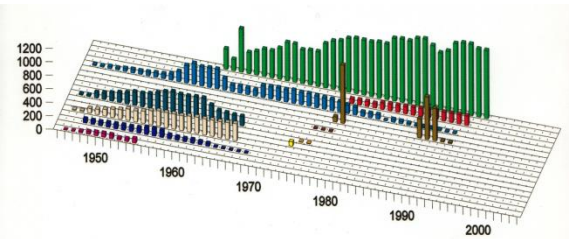

Figure 1. Raob/pibal inventory. From back to front, in megabytes; NMC, JMA, SPEC, FGGE/ECM, USAF, TD54, TWERLE, GATE, USCR, TD53, CARDS.

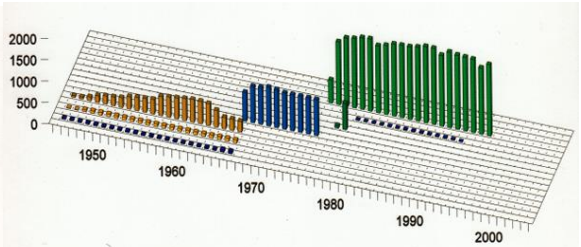

Figure 3. Land surface inventory. From back to front, in megabytes; NMC, ICEB, FGGE, USAF, TD13, TD14, USSR.

The components of each datatype were converted to WMO standard BUFR formats and assembled in a UNIX file system database structure. A consolidation system was developed to extract synoptic data from the database and assemble synoptic assimilation files for the reanalysis. The assembly system is diagramed below left, and the consolidated assimilation datasets shown graphically below right. A version of this system evolved over several years to perform this function in NCEP operations for ingest and preprocessing of all observations into the NCEP data assimilation and forecasting functions. The new BUFR database was implemented into operations in March 1997, as the 50 year R1 reanalysis was completing. The extension of R1 has been carried out at NCEP to the present day. The operational BUFR database has replaced the original prototype to supply observations to the R1 extension, otherwise known as CDAS.

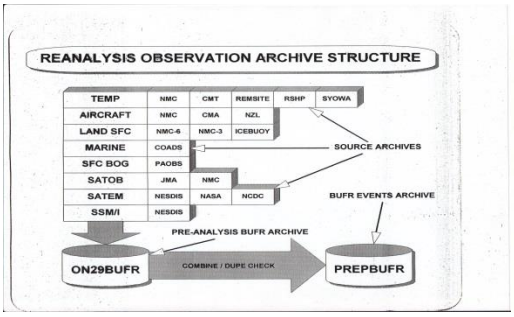

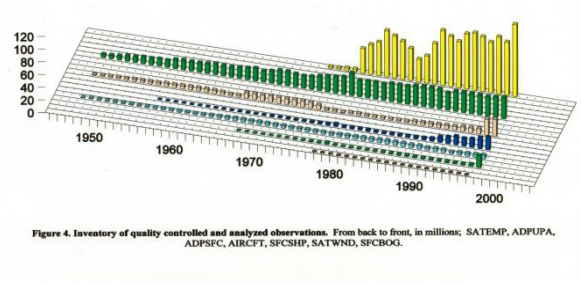

Figure 4. Inventory of quality controlled and analyzed observations. From back to front, in millions; SATEMP, ADPUPA, ADPSFC, AIRCFT, SFCSHP, SATWND, SFCBOG.

The NCEP Reanalysis Database is augmented with new observations from the BUFR database every day. Storing and using high resolution satellite data, staring around 1998 was challenging because of the sheer magnitude of the new datasets. The charts below illustrate the increase in and composition of NCEP data ingest from FGGE through 2009. Specific types of data added through the period are shown in the observation timeline below right. Thanks to an excellent tape archive system developed at NCEP over the past 20 years, the entire archive of GR1

reanalysis observation data has been saved intact, along with updates making corrections and additions over the years covered.

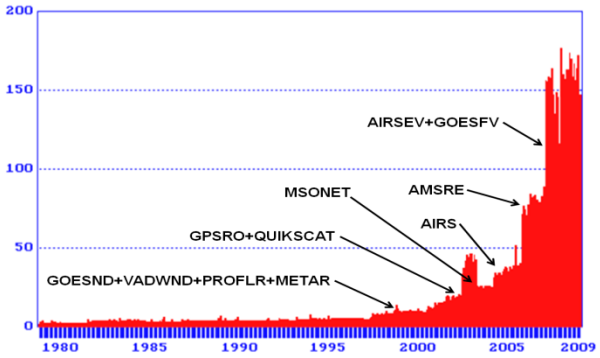

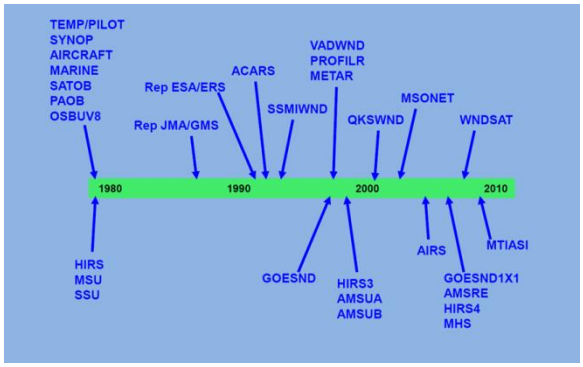

The GR1 database has been upgraded over time into modern NCEP/BUFR formats with improvements such as radiosonde drift and extended aircraft information, etc. New projects are starting at NCEP to reanalyze as far in the past as is useful for climate research. Several projects have analyzed surface obs back into the 19th century. NCEP plans to reanalyze back to at least 1948, in order to replace and update the GR1/CDAS with a third generation ensemble based reanalysis for advanced climate research and monitoring. The pilot for this will use the updated GR1 datasets, and with other historical dataset archives produced from other center's re-analyses, as they are available. NCEP is also focused on exchanging feedback information with other groups and products.

GR1 Observation Database Contributions to Other Reanalysis Projects

A number of reanalysis projects carried out around the world have directly benefitted from the work that went into creating the NCEP reanalysis observation archive for GR1. Additional reanalysis projects at NCEP, including GR2, NARR, and CFSR, all used the GR1 observation database. The ECMWF ERA40/ERAI/ERACLIM projects used significant amounts of the GR1 observations, 1957-1994. The JMA JRA25/JRA55 projects used NCEP and ERA40 datasets containing the GR1 datasets. MERRA1 and MERRA2 reanalysis projects at NASA/GMAO used the GR1/CDAS archive as the bulk of the conventional datasets. The ASR project at OSU downloaded the entire GR1 archive 1979-2014 as observations for reanalysis of the Arctic region. Below are references describing some of the prominent reanalysis projects which have used the GR1 datasets, and who provided constructive feedback.

Kalnay E, Kanamitsu M, Kirtler R, Collins W, Deaven D, Gandin L, IredellM, SahaS,WhiteG,WoollenJ, ZhuY,ChelliahM,EbisuzakiW, Higgins W, Janowiak J, Mo KC, Ropelewski C, Wang J, Leetma A, Reynolds R, Jenne R, Joseph D. 1996. The NCEP/NCAR 40-year reanalysis project. *Bull. Amer. Meteorol. Soc.* **77**: 437–471
.

Onogi K, Tsutsui J, Koide H, Sakamoto M, Kobayashi S, Hatsushika H, Matsumoto T, Yamazaki N, Kamahori H, Takahashi K, Kadokura S, Wada K, Kato K, Oyama R, Ose T, Mannoji N, Taira R. 2007. The JRA-25 Reanalysis. *J. Meteor. Soc. Japan* **85**: 369–432.

Saha S, Moorthi S, Pan H-L, Wu X, Wang J, Nadiga S, Tripp P, Kistler R, Woollen J, Behringer D, Liu H, Stokes D, Grumbine R, Gayno G, Hou Y-T, Chuang H-Y, JuangH-MH, Sela J, Iredell M, Treadon R, Kleist D, vanDelst P, Keyser D, Derber J, Ek M, Meng J, WeiH, YangR, Lord S, van den Dool H, Kumar A, Wang W, Long C, Chelliah M, Xue Y, Huang B, Schemm J-K, Ebisuzaki W, Lin R, Xie P, Chen M, Zhou S, Higgins W, Zou C-Z, Liu Q, Chen Y, Han Y, Cucurull L, Reynolds RW, Rutledge G, Goldberg M. 2010. The NCEP Climate Forecast System Reanalysis. *Bull. Amer.Meteorol. Soc.* **91**: 1015–105

Rienecker MM, Suarez MJ, Gelaro R, Todling R, Bacmeister J, Liu E, Bosilovich MG, Schubert SD, Takacs L, Kim G-K, Bloom S, Chen J, Collins D, Conaty A, da Silva A, Gu W, Joiner J, Koster RD, Lucchesi R, Molod A, Owens T, Pawson S, Pegion P, Redder CR, ReichleR,Robertson FR,Ruddick AG,SienkiewiczM,Woollen J. 2011. MERRA – NASA's Modern-Era Retrospective Analysis for Research and Applications. *J. Climate*, DOI: 10.1175/JCLI-D-11-00015.1.

Uppala SM, Kallberg PW, Simmons AJ, Andrae U, Da Costa Bechtold V, Fiorino M, Gibson JK, Haseler J, Hernandez A, Kelly GA, Li X, Onogi K, Saarinen S, Sokka N, Allan RP, Andersson E, Arpe K, Balmaseda MA, Beljaars ACM, Van De Berg L, Bidlot J, Bormann N, Caires S, Chevallier F, Dethof A, Dragosavac M, Fisher M, FuentesM, Hagemann S, Holm E, Hoskins BJ, Isaksen L, Janssen PAEM, Jenne R, McNally AP, Mahfouf JF, Morcrette J-J, Rayner NA, Saunders RW, Simon P, Sterl A, Trenberth KE, Untch A, Vasiljevic D, Viterbo P, Woollen J. 2005. The ERA-40 re-analysis. *Q. J. R. Meteorol. Soc.* **131**: 2961–3012.